Liquid Crystals
Publication details, including instructions for authors and subscription information:
http://www.informaworld.com/smpp/title~content=t713926090

Dynamics of the Goldstone mode near the point of polarization sign reversal in ferroelectric liquid crystal-aerosil mixtures

StanisŁaw A. Różański[a]; Jan Thoen[a]
[a] Laboratorium voor Akoestiek en Thermische Fysica, Departement Natuurkunde en Sterrenkunde, Katholieke Universiteit Leuven, B-3001 Leuven, Belgium

To cite this Article Różański, StanisŁaw A. and Thoen, Jan(2005) 'Dynamics of the Goldstone mode near the point of polarization sign reversal in ferroelectric liquid crystal-aerosil mixtures', Liquid Crystals, 32: 8, 1013 — 1020
To link to this Article: DOI: 10.1080/02678290500248202
URL: http://dx.doi.org/10.1080/02678290500248202

Liquid Crystals, Vol. 32, No. 8, August 2005, 1013–1020

Dynamics of the Goldstone mode near the point of polarization sign reversal in ferroelectric liquid crystal–aerosil mixtures

STANISŁAW A. RÓŻAŃSKI and JAN THOEN*

Laboratorium voor Akoestiek en Thermische Fysica, Departement Natuurkunde en Sterrenkunde, Katholieke Universiteit Leuven, Celestijnenlaan 200D, B-3001 Leuven, Belgium

(*Received 6 January 2005; in final form 12 May 2005; accepted 19 May 2005*)

Dielectric spectroscopy was used to study the influence of random disorder in aerosil–ferroelectric liquid crystal dispersions on the dynamics of the Goldstone mode near the point of polarization sign reversal and the relaxation rate and dielectric strength of the collective modes. In general, the dielectric strength and the relaxation frequency of the Goldstone mode decrease, in comparison with the bulk, with increasing aerosil density near a point of polarization sign reversal. However, the characteristic frequency of the Goldstone mode varies with silica density in an opposite manner on each side of this point. This can be explained as a different sensitivity on the spatial confinement of different molecular conformers above and below the point of polarization sign reversal. The experimental results of temperature and frequency dependence of the complex dielectric constant are compared with predictions of the generalized Landau model for ferroelectric liquid crystals.

1. Introduction

The inversion of the sign of the spontaneous polarization ($\mathbf{P}_s$) is an interesting effect observed recently in several liquid crystal materials. This phenomenon was already known in single-component mesogens [1–14], two-component mixtures [15–17] and polymer systems [18]. The ferroelectric liquid crystal *S*-(-)-2-methylbutyl 4-*n*-nonanoyloxybiphenyl-4′-carboxylate is a member of the 2-methylbutyl 4-alkanoyloxybiphenyl-4′-carboxylate series [1, 2], that shows polarization sign reversal. Several different experimental techniques have been applied to explain the origin of this fact: elipsometric measurements on freely suspended films [6–8], electro-optic measurements of $\mathbf{P}_s$, rotational viscosity, tilt angle, helical pitch and rotatory power [9–12], dielectric spectroscopy [9, 12], field-dependent pyroelectric techniques [13], and polarized FTIR spectroscopy [14].

In the smectic A phase (SmA) of ferroelectric liquid crystals (FLCs) the molecules are oriented perpendicular to the smectic layers and rotate freely around their long molecular axis; as a result spontaneous polarization is not observed. However, in the ferroelectric smectic C* phase (SmC*) the symmetry reduces from D_∞ to C_2 with the chiral molecules tilted with respect to the normal to the smectic layers. The observed local ferroelectricity in the SmC* phase is an effect of the hindered rotation of the molecules around the molecular long axis and an ordering of the molecular short axes which bear electric dipole moments. As a consequence of a chirality helical superstructure is created in the SmC* phase and the spontaneous polarization rotates from layer to layer, leading to the cancelling of the average polarization in the sample. The tilt angle is considered as a primary order parameter and spontaneous polarization as a secondary order parameter. These two-component order parameters play an important role in the theoretical description of the dynamic properties of the SmA and the SmC* phases on the basis of a generalized Landau expansion of the free energy density of the system [19–23].

To explain the polarization sign reversal in the SmC* phase several modifications were introduced to the theoretical calculations and also some different models were proposed [1, 2, 24–29]. In one of these models, the vanishing of the polarization in certain FLCs at a characteristic temperature is explained as a consequence of the presence of at least two structural conformers, inter-convertible via an activation barrier [1, 2]. The temperature induced sign inversions of $\mathbf{P}_s$ can also be elucidated taking into account a possible competition between polar and quadrupolar ordering in the potential describing rotation of the molecule about the molecular long axis [24–27]. Moreover, the origin and

*Corresponding author. Email: Jan.Thoen@fys.kuleuven.be

Liquid Crystals
ISSN 0267-8292 print/ISSN 1366-5855 online © 2005 Taylor & Francis
http://www.tandf.co.uk/journals
DOI: 10.1080/02678290500248202

sign of $\mathbf{P}_s$ can be derived if an individual molecule is modelled qualitatively by a surface of constant molecular mean field [28, 29]. However, in induced liquid crystalline SmC* phases, the sign inversion of the spontaneous polarization can only be explained taking into account different chiral interactions between the guest and host molecules [15].

In FLCs two collective dynamic modes can be observed. In the SmA phase the soft mode appears, which is connected with the amplitude changes of the order parameter. In the SmC* phase, as well as the soft mode, the Goldstone mode related with the phase changes of the order parameter becomes visible. These collective modes are very sensitive to external fields and geometric restrictions. The influence of the confinement on the dynamics of the collective modes has been studied using dielectric spectroscopy in systems such as polymer dispersed FLCs [30], porous membranes [31–33], porous glasses [34, 35], aerogels [36], aerosil–FLC dispersions [37–39] and planar cells [40–44]. In aerosil–FLC dispersions, in particular, the random disorder can be introduced in a controlled way, which provides information about physical mechanisms leading to the reduced dynamics of the collective modes in confinement.

It has been shown in a previous experiment [39] that with increasing aerosil density the dielectric strength of the Goldstone and the soft mode decreases and for some critical silica density the Goldstone mode disappears completely. The characteristic frequency of the Goldstone mode slightly increases. The frequency degeneracy at the SmA–SmC* phase transition is removed in the presence of aerosils and the frequency gap increases with increasing silica density. However, less is known about the influence of the aerosil particles on the polarization sign reversal appearing in the investigated smectogen. The chiral centre of the molecule, responsible for the spontaneous polarization, is located in the flexible alkyl chain far away from the aromatic core. For this reason it can be expected that this system should be sensitive to spatial confinement also near the point of the polarization sign reversal.

In this study the temperature, frequency and silica density dependence of the complex dielectric constant of the Goldstone mode near a point of the polarization sign reversal is investigated. Possible mechanisms responsible for the observed changes of the dynamics of the Goldstone mode near a point of polarization sign reversal are discussed on the basis of existing models. The experimental results for bulk FLC and aerosil–FLC dispersions are compared with predictions of the generalized Landau model.

2. Experimental

To investigate the influence of disorder on the collective relaxation processes near the SmA–SmC* phase transition, and in the point of polarization sign reversal, several mixtures of hydrophilic aerosil 300 (Degussa Corp.) with the ferroelectric liquid crystal *S*-(-)-2-methylbutyl 4-*n*-nonanoyloxybiphenyl-4′-carboxylate (denoted as IS-2424) (AWAT Sp. z o.o.) were prepared. The structural formula of this FLC, with the two possible conformers (*a*) and (*b*) for the *S*-2-methylbutyl moiety, is shown in figure 1. It is known that the ferroelectric liquid crystal IS-2424, with the phase transition temperature sequence Cr 312.15 K SmC* 315.65 K SmA 332.65 K I, possesses a polarization sign inversion at a temperature of about 292 K [1, 9–11]. The ferroelectric SmC* phase appears in a broad temperature range and can be easily supercooled to about 265 K. The value of the helical pitch for this material is about 3 μm near the SmA–SmC* phase transition and the $\mathbf{P}_s$ is about $2\,\mathrm{nC\,cm^{-2}}$ at the maximum of the temperature dependence [9].

The spherically-shaped primary particles of the hydrophilic aerosil have a diameter of about 7 nm and a specific surface area of about $300\,\mathrm{m^2\,g^{-1}}$. The surfaces of the silica particles are covered by hydroxyl groups and in solution can form hydrogen-bonded networks. Depending on the silica density there can be a change from a soft gel-like system to a fragile structure comparable to aerogels [37, 45]. Aerosil–FLC mixtures with density $\rho_s = 0.025$, 0.05, 0.08, 0.15 and $0.2\,\mathrm{g\,cm^{-3}}$ were prepared using the solvent method described previously [39]. The aerosil density ρ_s in the mixtures was calculated from the formula: $\rho_s = (m_s/m_{LC})\rho_{LC}$, where m_s and m_{LC} are the masses of aerosil and liquid crystal, respectively, and $\rho_{LC} \sim 1\,\mathrm{g\,cm^{-3}}$ is the density of liquid crystal.

Real $\varepsilon'(\omega)$ and imaginary $\varepsilon''(\omega)$ parts of the complex dielectric permittivity $\varepsilon^*(\omega) = \varepsilon'(\omega) - i\varepsilon''(\omega)$ were measured in the frequency range from 10^{-2} Hz to about 10 MHz using a Novocontrol broadband dielectric spectrometer with an Alpha high resolution dielectric/impedance analyser and an active sample cell. The gold plated electrodes separated by 50 μm glass fibre spacers formed a measuring capacitor, which was filled with liquid crystal. It is known that on the gold-plated surfaces the liquid crystal molecules can take a planar orientation [46]. The FLC investigated undergoes a direct transition from the isotropic to the SmA phase with decreasing temperature which does not lead to a good orientation of the liquid crystal. Therefore, the mesogen was slowly heated and cooled several times across the isotropic–SmA phase transition, which improved the orientation of the bulk FLC. However,

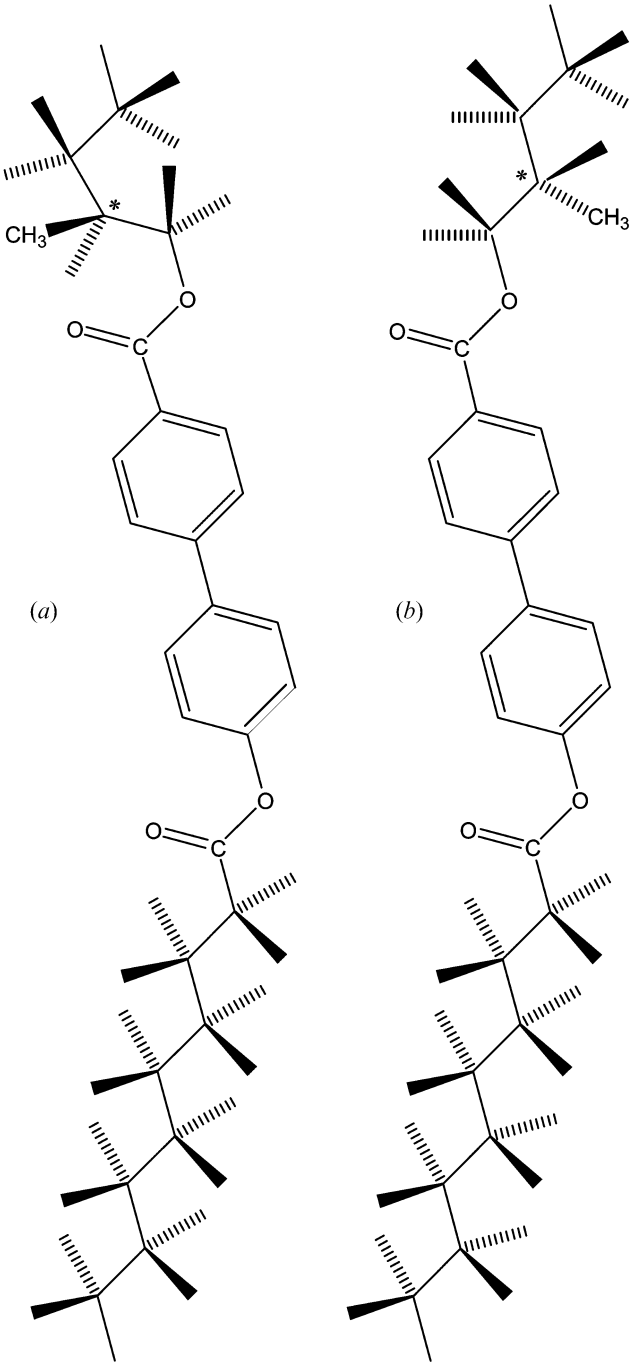

Figure 1. Sructural formula of the ferroelectric liquid crystal *S*-(-)-2-methylbutyl 4-*n*-nonanoyloxybiphenyl-4′-carboxylate with the two possible conformers (*a*) and (*b*) for the *S*-2-methylbutyl moiety.

with increasing aerosil density the samples remain more viscous and are aligned with difficulty, even in a high magnetic field [37, 38]. The measurements were performed in the temperature range from 336 K to 265 K on cooling the sample, with temperature steps of about 50 mK near the SmA–SmC* phase transition, and about 0.5 K near the point of polarization sign reversal, to obtain the appropriate temperature resolution.

In the range of frequency investigated, only one relaxation process related with the soft mode appears in the paraelectric SmA phase, and dielectric spectra were evaluated using superposition of one Harviliak–Negami relaxation function [47] and a conductivity contribution. However, in the SmC* phase the soft mode splits into the Goldstone mode, and the soft amplitude mode and the dielectric spectra were fitted with two Havriliak–Negami functions and a conductivity contribution:

$$\varepsilon^*(\omega, T \geq T_{CA}) = \varepsilon_\infty + \frac{\Delta\varepsilon_s}{\left[1 + (i\omega\tau_s)^{1-\alpha_S}\right]^{\beta_S}} - \frac{i\sigma_0}{\varepsilon_0\omega^n} \qquad (1a)$$

$$\varepsilon^*(\omega, T \geq T_{CA}) = \varepsilon_\infty + \frac{\Delta\varepsilon_s}{\left[1 + (i\omega\tau_s)^{1-\alpha_S}\right]^{\beta_S}} + \frac{\Delta\varepsilon_G}{\left[1 + (i\omega\tau_G)^{1-\alpha_G}\right]^{\beta_G}} - \frac{i\sigma_0}{\varepsilon_0\omega^n} \qquad (1b)$$

where parameters characterizing the relaxation process are the relaxation times τ and the relaxation strength $\Delta\varepsilon$. The exponents α and β describe broadening and asymmetry of the relaxation time distribution, respectively. ε_∞ is the high frequency limit of the permittivity and ε_0 is the permittivity of free space. The conductivity contribution expressed by the term $\frac{i\sigma_0}{\varepsilon_0\omega^n}$ dominates in the low frequency range where σ_0 is the Ohmic conductivity and n a fitting parameter.

3. Results and discussion

Figure 2 presents a sequence of diagrams of the frequency dependence of the imaginary part of the dielectric function for the bulk FLC at different temperatures close to the SmA–SmC* phase transition. The observed relaxation processes and conductivity contribution were separated by fitting the dielectric data with the Havriliak–Negami function equation (1). In the SmA phase only one relaxation process is observed and assigned to the double degenerated soft mode, figure 2 (*a*). However, close to T_{AC} in the SmC* phase two modes start to contribute to the dielectric response and the relaxation process splits into the Goldstone mode and the soft amplitude mode, figure 2 (*b*). With decreasing temperature the dielectric strength of the soft mode rapidly decreases and is partially hidden by the Goldstone mode, figure 2 (*c*). Apart from the Goldstone

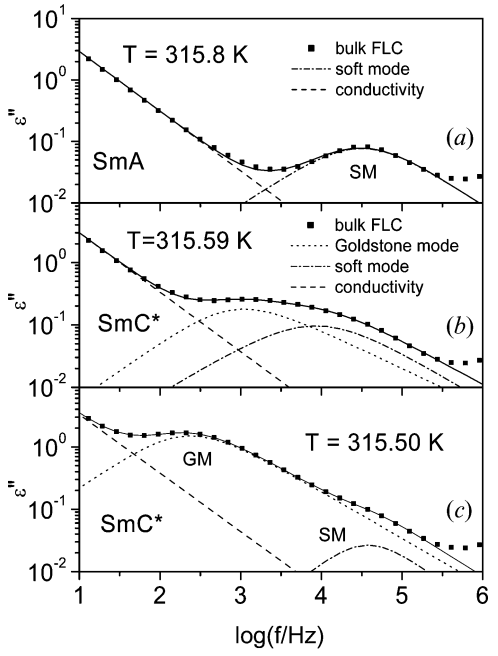

Figure 2. Frequency dependence of the imaginary part of the dielectric function near the SmA–SmC* phase transition. In the SmA phase only the soft mode is visible (*a*). In the SmC* phase close to the phase transition the Goldstone mode and the soft modes are present (*b*). At some distance from the transition the Goldstone mode dominates (*c*).

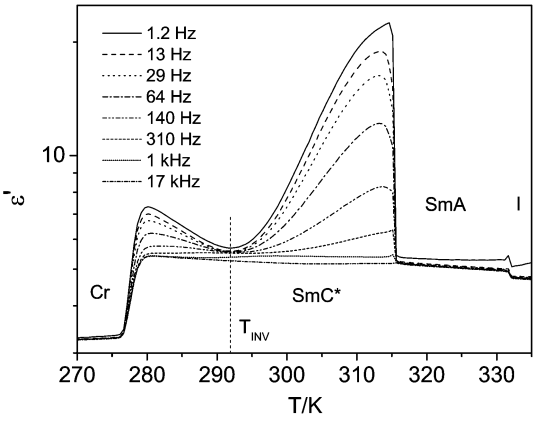

Figure 3. Temperature dependence of the dielectric constant near the SmA–SmC* phase transition and near the point of polarization sign inversion at chosen frequencies.

mode, therefore, it is also possible to observe the contribution from the soft mode if the measurements are performed close enough to the phase transition. However, farther away from the phase transition the domination of the Goldstone mode can be suppressed by a bias field, and only in this way is the separation of both modes possible.

Figure 3 shows the temperature dependence of the dielectric constant $\varepsilon'(\omega)$ for some frequencies in the range from 1 Hz to about 20 kHz. For low frequencies near the SmA–SmC* phase transition, the Goldstone mode dominates in the SmC* phase and its dielectric constant decreases with increasing frequency. However, for higher frequencies above 1 kHz only the dielectric response related with the soft mode and ε_∞ is present. Moreover, at low frequencies the dielectric constant also decreases with decreasing temperature to a value comparable to ε_∞ in a point of polarization sign reversal. Below the T_{INV} the dielectric constant related with the Goldstone mode increases again and after approaching a maximum, which is much lower than near the SmA–SmC* transition, tends to zero with the crystallization of the sample.

Figure 4 shows the temperature evolution of the dielectric losses of the Goldstone mode near the point of the polarization sign reversal. Starting from the SmA–SmC* phase transition temperature T_{AC}=315.65 K, the dielectric losses increase with decreasing temperature, figure 4 (*a*), and after approaching a maximum at 311.84 K decrease again, figure 4 (*b*). With further temperature decrease it reaches a minimum at a temperature of about 291.16 K. The exact temperature

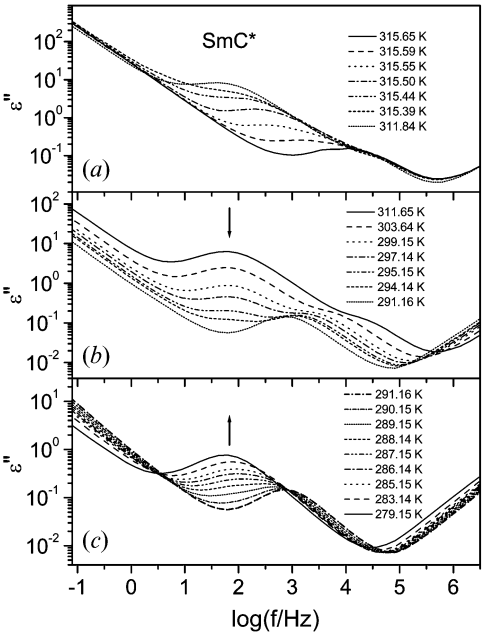

Figure 4. Frequency and temperature evolution of the dielectric losses related to the Goldstone mode near the point of polarization sign reversal: (*a*) 315.65→311.84 K, (*b*) 311.65→291.16 K, (*c*) 291.16→279.15 K.

of the polarization sign inversion $T_{INV}=291.65\,K$ was determined from inspection of the dielectric spectra and observations under the polarizing microscope. Below T_{INV} the dielectric losses increase once more, figure 4 (*c*). The temperature dependence of the dielectric losses of the Goldstone mode reflects the temperature dependence of the spontaneous polarization $\mathbf{P}_s$ for this compound.

Figure 5 presents the influence of silica density on the temperature dependence of the dielectric constant at a frequency where the dielectric response from the Goldstone mode dominates. With increasing aerosil density the dielectric constant decreases both near the SmA–SmC* phase transition and below the point of polarization sign reversal. For high densities only the dielectric response from the high frequency dielectric permittivity is present and the Goldstone mode disappears. The changes in the value of the dielectric constant are related to the influence of the silica particles on the dynamics and on the dielectric strength of the Goldstone mode.

The theoretical model predicts that in the SmA phase the inverse of the dielectric strength $\Delta\varepsilon_{s,A}$ and the relaxation frequency $f_{s,A}$ of the soft mode decreases linearly with temperature and are given by the following expressions [19–23]:

$$\varepsilon_0\Delta\varepsilon_{s,A}=\frac{\varepsilon^2C^2}{a_0(T-T_{AC})+(K_3-\varepsilon\mu^2)q_0^2} \tag{2}$$

$$f_{s,A}=\frac{a_0(T-T_{AC})+\left(K_3-\varepsilon\mu^2\right)q_0^2}{2\pi\gamma_{s,A}} \tag{3}$$

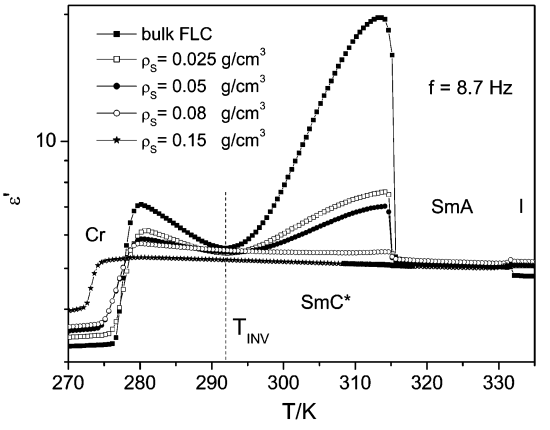

Figure 5. Temperature dependence of the dielectric constant near the SmA–SmC* phase transition and near the point of polarization sign reversal for the bulk FLC and for different aerosil densities.

where a_0 is the phenomenological constant of the Landau expansion of the free energy density, $\gamma_{s,A}$ is the rotational viscosity of the soft mode in the SmA phase, μ and C are coefficients of the flexoelectric and piezoelectric bilinear coupling, respeclively, K_3 is the twist elastic constant, while q_0 is the wave vector of the pitch at T_{AC}. ε is the dielectric constant of the system in the high frequency limit [19] and can be taken equal to ε_∞.

The product of equations (2) and (3) is temperature independent and can be expressed as:

$$\Delta\varepsilon_{s,A}f_{s,A}=\frac{\varepsilon^2C^2}{2\pi\varepsilon_0\gamma_{s,A}} \tag{4}$$

Moreover, a comparable expression can be obtained from the generalized Landau model for the soft mode in the SmC* phase [20]:

$$f_s=\frac{X}{2\pi\gamma_s} \tag{5}$$

$$\varepsilon_0\Delta\varepsilon_s=\frac{1}{2X}\left(\frac{b_3}{b_7}\right)^2 \tag{6}$$

$$\Delta\varepsilon_s f_s=\frac{1}{4\pi\varepsilon_0\gamma_s}\left(\frac{b_3}{b_7}\right)^2 \tag{7}$$

where γ_s is the rotational viscosity of the soft mode in the SmC* phase, while b_3, b_7 and X are constants depending on the material parameters.

The value of the product of $\Delta\varepsilon_{s,A}$ and $f_{s,A}$ in the SmA phase obtained experimentally from dielectric measurements for the bulk FLC approximates to 6×10^3 Hz near the SmA–SmC* phase transition. For temperatures close to the phase transition the tilt angle and polarization are small and the linear relation between these quantities can be written as $\mathbf{P}_s/\theta\approx\varepsilon C$ [48]. Because the $\mathbf{P}_s$ and θ are known for this compound [1, 9] the soft mode rotational viscosity $\gamma_{s,A}$ in the SmA phase can be estimated. The value of $\gamma_{s,A}$ calculated from equation (4) is about $0.02\,N\,s\,m^{-2}$.

The Goldstone mode dielectric strength $\Delta\varepsilon_G$ and characteristic relaxation frequency f_G can be expressed in terms of spontaneous polarization $\mathbf{P}_s$, tilt angle θ and the wave vector of the pitch q in the form [21]:

$$\Delta\varepsilon_G=\frac{1}{2\varepsilon_0K_3q^2}\left(\frac{\mathbf{P_s}}{\theta}\right)^2 \tag{8}$$

$$f_G=\frac{K_3q^2}{2\pi\gamma_G} \tag{9}$$

From equations (8) and (9) an expression for the

product of $\Delta\varepsilon_G$ and f_G can be derived:

$$\Delta\varepsilon_G f_G = \frac{1}{4\pi\varepsilon_0\gamma_G}\left(\frac{\mathbf{P}_s}{\theta}\right)^2 \quad (10)$$

Equation (10) shows that the product of the dielectric strength and the relaxation frequency of the Goldstone mode is expected to be proportional to $(\mathbf{P}_s/\theta)^2$. Figure 6 presents the experimentally determined temperature dependence of this product for different densities of the hydrophilic aerosil particles. Near the SmA–SmC* phase transition this quantity attains a maximum. However, with further decrease of temperature it does not saturate with $\mathbf{P}_s/\theta$. Two reasons may be responsible for this dependence. One is related to the rather unusual temperature dependence of the spontaneous polarization in the investigated FLC compound. After approaching a maximum near the SmA–SmC* phase transition $\mathbf{P}_s$ decreases with decreasing temperature, and at the temperature T_{INV} a sign inversion of $\mathbf{P}_s$ is observed [1, 9, 10]; at this point $\mathbf{P}_s=0$. In the model, which explains the $\mathbf{P}_s$ inversion as a result of a competition between at least two different molecular conformers, the temperature dependence of $\mathbf{P}_s$ is described by the equation:

$$\boldsymbol{P}_s = \left\{ P_A \exp\left(-\frac{\Delta E}{k_B T}\right) + P_B\left[1-\exp\left(-\frac{\Delta E}{k_B T}\right)\right]\right\}_{(T_{AC}-T)\alpha} \quad (11)$$

where P_A, P_B, ΔE and α are fit parameters while k_B is the Boltzmann constant [1, 2]. Below this point the absolute value of the polarization again increases with further decrease of temperature. The temperature dependence of the tilt angle θ shows no anomaly in this temperature range [9, 11]. Another reason for this dependence may be connected with the temperature dependence of the rotational viscosity of the Goldstone mode γ_G, which should be expected to increase with decreasing temperature.

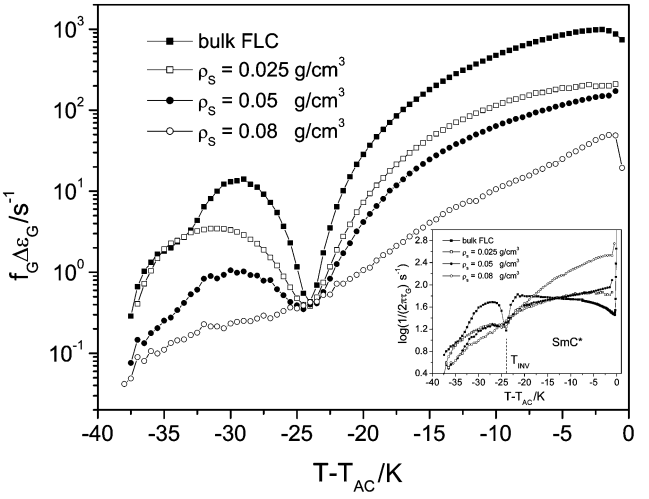

Figure 6. Temperature dependence of the product of dielectric strength $\Delta\varepsilon_G$ and the characteristic frequency f_G of the Goldstone mode near the point of polarization sign reversal for some aerosil densities. The inset gives the characteristic Goldstone mode frequency as a function of temperature.

Additionally, with increasing density of the aerosil particles a decrease of the $\Delta\varepsilon_G f_G$ product is observed. This can be related to an increase in viscosity of the system as a result of the hydrogen-bonded network structure formed by hydrophilic aerosil particles in the liquid crystal. According to equation (10), the product of $\Delta\varepsilon_G$ and f_G should be equal to zero at the point of polarization sign inversion. The experimentally determined value of this product differs slightly from zero, which can be related to an incomplete compensation of the spontaneous polarization, resulting from too large steps in the temperature changes during dielectric measurements.

In the inset in figure 6 the temperature dependence of the characteristic frequency of the Goldstone mode $f_G=1/(2\pi\tau_G)$ for several aerosil densities is presented. With increasing silica density the f_G increases near the SmA–SmC* phase transition, probably as a results of helix distortion caused by interaction with the hydrogen-bonded network formed in the FLC. For the bulk FLC and for low silica densities the f_G is nearly temperature independent. However, with increasing aerosil density the frequency starts to decrease with decreasing temperature. Moreover, at the temperature of polarization sign reversal T_{INV}, a characteristic dip in the frequency is observed related to the disappearance of the spontaneous polarization. The dip diminishes with increasing silica density. At this point the Goldstone mode cannot be activated because there is no coupling between polarization and electric field, and the relaxation time increases theoretically to infinity. The characteristic frequency f_G is lower on both sides of T_{INV} in comparison with the bulk. Additionally, above T_{INV} the sequence of f_G is inverted compared with those below T_{INV}, with increasing aerosil density.

As mentioned earlier, the chiral centre responsible for the spontaneous polarization is located on the flexible alkyl chain far from the aromatic core of the molecule and should be sensitive to the distortions introduced to the system by silica particles. If one assumes this model (which explains the $\mathbf{P}_s$ inversion as a competition between at least two molecular conformers with different mean orientations of the molecular dipole moment with respect to the tilt plane), it is reasonable to conclude that the hydrogen-bonded network formed by

silica particles can affect these molecular species differently. In this situation, changes in the dynamics of the Goldstone mode above and below the point of polarization sign inversion can be manifested in the inversion of the sequence of the characteristic frequencies with increasing silica density.

For higher aerosil densities the hydrogen bonds between aerosil particles and FLC molecules cannot be excluded from having some kind of influence on the collective dynamic of the system. The structural formulae of the FLC molecule shown in figure 1 suggest that aerosil particles covered by hydroxyl groups can form hydrogen bonds with electronegative oxygen heteroatoms present in the FLC molecule. Oxygen atoms related to linking groups are located near the rigid biphenyl core of the molecule, and bind the rather long aliphatic chain on one side of the molecule and the moeity with a chiral centre on the other side. Hydrogen bonding of the OH groups of the aerosil particles to the oxygen atoms in linking groups can influence the rotational freedom of the chiral centre relative to the long axis of the molecule, or can influence the flexibility of the aliphatic chain. How these hydrogen bonds really influence the dynamic of the FLC molecules may be established by an analysis of the IR spectra of the aerosil–FLC composite and should possibly be done in future experiments.

Figure 7 shows a plot of the inverse of the dielectric strength $1/\Delta\varepsilon_s$ of the soft mode as a function of $T-T_{AC}$, both above and below the SmA–SmC* phase transition temperature. The solid line represents a linear fit of the experimental data with the function $1/\Delta\varepsilon_s=a(T-T_{AC})+b$ in the SmC* phase, where a and b are fit parameters. The temperature dependence of $1/\Delta\varepsilon_s$ for bulk FLC is linear in the SmC* phase and non-linear in the SmA phase. From equation (2) it arises that $1/\Delta\varepsilon_{s,A}$ linearly decreases with temperature if the temperature dependence of the other parameters are negligible. Therefore, the non-linear variation of $1/\Delta\varepsilon_{s,A}$ can be explained probably as a temperature change of the twist to piezo-energy ratio [49]. However, the slope of $1/\Delta\varepsilon_s$ in the SmC* phase decreases with increasing silica density (see inset in figure 7). This tendency of decreasing slope with increasing aerosil density may be connected with the influence of the silica particles on the material parameters related by equation (6). Moreover, with increasing silica density the Goldstone mode is not completely quenched by the hydrogen-bonded network formed in the FLC, which may influence the separation of the soft mode in the SmC* phase. Also the dynamic properties of the soft mode in the SmA–SmC* phase transition are significantly modified by aerosil particles [37–39].

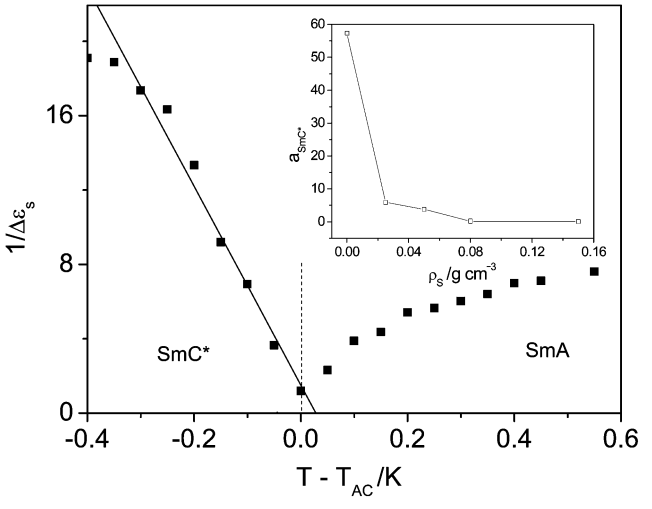

Figure 7. Temperature dependence of the inverse of the soft mode dielectric strength near the SmA–SmC* phase transition in the bulk FLC. The inset shows the aerosil density dependence of the slope in the SmC* phase.

4. Conclusions

Dielectric measurements reveal that only close to the SmA–SmC* phase transition does the relation between spontaneous polarization $\mathbf{P}_s$ and tilt angle θ agree well with theoretical predictions. The disappearance of the Goldstone mode at T_{INV} indicates the vanishing of $\mathbf{P}_s$ at this temperature. This unusual behavior suggests that $\mathbf{P}_s$ cannot be considered as a good order parameter in the investigated smectogen, except near to the SmA–SmC* phase transition. The dielectric strength, characteristic frequency and product of these quantities for the Goldstone mode show a pronounced minimum in temperature dependence at the point of polarization sign reversal. The temperature dependence of the inverse of the soft mode dielectric strength is significantly influenced by aerosil particles in comparison with the bulk. Above the point of polarization sign reversal the characteristic frequency of the Goldstone mode decreases with decreasing aerosil density. However, below this point the frequency decreases with increasing silica density. The observed effect probably arises from the different influence of the hydrogen-bonded network of the aerosil particles on the two different molecular conformers present above and below a point of polarization sign reversal. The influence of the aerosil particles on the dynamics of the Goldstone mode near the SmA–SmC* phase transition differs from the dynamics near the point of the polarization inversion. These differences are mainly related to the unusual temperature dependence of the spontaneous polarization in the investigated smectogen.

Acknowledgments

This work has been supported by the National Fund for Scientific Research Flanders, Belgium (FWO, project G.0246.02). S.A.R. acknowledges the receipt of a senior postdoctoral fellowship from the Research Council of K.U.Leuven.

References

[1] J.W. Goodby, E. Chin, J.M. Geary, J.S. Patel, P.L. Finn. *J. chem. Soc. Faraday Trans.*, **83**, 3429 (1987).
[2] J.S. Patel, J.W. Goodby. *Philos. Mag. Lett.*, **55**, 238 (1987).
[3] S. Saito, K. Murashiro, M. Kikuchi, D. Demus, T. Inukai, M. Neundorf, S. Diele. *Ferroelectrics*, **147**, 367 (1993).
[4] Y. Mieda, H. Hoshi, Y. Takanishi, H. Takezoe, B. Žekš. *Phys. Rev. E*, **67**, 021701 (2003).
[5] D. Schlauf, Ch. Bahr, C.C. Huang. *Phys. Rev. E*, **55**, 4885 (1997).
[6] Ch. Bahr. *Mol. Cryst. liq.Cryst.*, **301**, 313 (1997).
[7] Ch. Bahr, C.J. Booth, D. Fliegner, J.W. Goodby. *Ferroelectrics*, **178**, 229 (1996).
[8] Ch. Bahr, C.J. Booth, D. Fliegner, J.W. Goodby. *Europhys. Lett.*, **34**, 507 (1996).
[9] R. Eidenschink, T. Geelhaar, G. Andersson, A. Dahlgren, K. Flatischler, F. Gouda, S.T. Lagerwall, K. Skarp. *Ferroelectrics*, **84**, 167 (1988).
[10] K. Skarp, F. Flatischler, S.T. Lagerwall. *Ferroelectrics*, **84**, 183 (1988).
[11] I. Muševič, I. Drevenšek, R. Blinc, S. Kumar, J.W. Doane. *Mol. Cryst. liq. Cryst.*, **172**, 217 (1989).
[12] K. Nakano, M. Ozaki, K. Yoshino. *Jpn. J. appl. Phys.* Part 1, **26**, Suppl. 26–2, 104 (1987).
[13] A.M. Glass, J.W. Goodby, D.H. Olson, J.S. Patel. *Phys. Rev. A*, **38**, 1673 (1988).
[14] W.G. Jang, C.S. Park, J.E. Maclennan, K.H. Kim, N.A. Clark. *Ferroelectrics*, **180**, 213 (1996).
[15] H. Stegemeyer, A. Sprick, M.A. Osipov, V. Vill, H.-W. Tunger. *Phys. Rev. E*, **51**, 5721 (1995).
[16] H. Stegemeyer, R. Meister, H.-J. Altenbach, D. Szewczyk. *Liq. Cryst.*, **14**, 1007 (1993).
[17] H. Stegemeyer, R. Meister, K.-H. Ellermann, H.-J. Altenbach, W. Sucrow. *Liq. Cryst.*, **5**, 667 (1992).
[18] G. Scherowsky, B. Brauer, K. Grunegerg, U. Muller, L. Komitov, S.T. Lagerwall, K. Skarp, B. Stebler. *Mol. Cryst. liq. Cryst.*, **215**, 257 (1992).
[19] C. Filipič, T. Carlsson, A. Levstik, B. Žekš, R. Blinc, F. Gouda, S.T. Lagerwall, K. Skarp. *Phys. Rev. A*, **38**, 5833 (1988).
[20] T. Carlsson, B. Žekš, C. Filipič, A. Levstik. *Phys. Rev. A*, **42**, 877 (1990).
[21] A. Levstik, Z. Kutnjak, C. Filipič, I. Levstik, Z. Bregar, B. Žekš, T. Carlsson. *Phys. Rev. A*, **42**, 2204 (1990).
[22] A. Levstik, T. Carlsson, C. Filipič, I. Levstik, B. Žekš. *Phys. Rev. A*, **35**, 3527 (1987).
[23] R. Blinc, B. Žekš. *Phys. Rev. A*, **18**, 740 (1978).
[24] B. Kutnjak-Urbanc, B. Žekš. *Liq. Cryst.*, **18**, 483 (1995).
[25] B. Urbanc, B. Žekš. *Liq. Cryst.*, **5**, 1075 (1989).
[26] M.A. Osipov, R. Meister, H. Stegemeyer. *Liq. Cryst.*, **16**, 173 (1994).
[27] R. Meister, H. Stegemeyer. *Ber. Bunsenges. Phys. Chem.*, **97**, 1242 (1993).
[28] D.J. Photinos, E.T. Samulski. *Science*, **270**, 783 (1995).
[29] D.M. Walba. *Advances in the Synthesis and Reactivity of Solids* Vol. 1, 173–235 (1991).
[30] E.P. Pozhidaev, D. Ganzke, V.Ya. Zyryanov, S.L. Smorgon, W. Haase. *Liq. Cryst.*, **29**, 1305 (2002).
[31] K.L. Sandhya, S. Krishna Prasad, D.S. Shankar Rao, Ch. Bahr. *Phys. Rev. E*, **66**, 031710 (2002).
[32] S.A. Różański, R. Stannarius, F. Kremer, S. Diele. *Liq. Cryst.*, **28**, 1071 (2001).
[33] S.A. Różański, R. Stannarius, F. Kremer. *IEEE Trans. Dielectrics and Electrical Insulation*, **8**, 488 (2001).
[34] L. Naji, F. Kremer, R. Stannarius. *Liq. Cryst.*, **25**, 363 (1998).
[35] F.M. Aliev, J. Kelly. *Ferroelectrics*, **151**, 263 (1994).
[36] H. Xu, J.K. Vij, A. Rappaport, N.A. Clark. *Phys. Rev. Lett.*, **79**, 249 (1997).
[37] Z. Kutnjak, S. Kralj, S. Žumer. *Phys. Rev. E*, **66**, 041702 (2002).
[38] Z. Kutnjak, G. Cordoyiannis, G. Nounesis. *Ferroelectrics*, **294**, 105 (2003).
[39] S.A. Różański, J. Thoen. *Liq. Cryst.*, **32**, 331 (2005).
[40] M. Škarabot, S. Kralj, R. Blinc, I. Muševič. *Liq. Cryst.*, **26**, 723 (1999).
[41] V. Novotná, M. Glogarová, A.M. Bubnov, H. Sverenyák. *Liq. Cryst.*, **23**, 511 (1997).
[42] Yu.P. Panarin, Yu.P. Kalmykov, S.T. Mac Lughadha, H. Xu, J.K. Vij. *Phys. Rev. E*, **50**, 4763 (1994).
[43] T. Povše, I. Muševič, B. Žekš, R. Blinc. *Liq. Cryst.*, **14**, 1587 (1993).
[44] K. Kondo, H. Takezoe, A. Fukuda, E. Kuze. *Jpn. J. appl. Phys.*, **21**, 224 (1982).
[45] G.S. Iannacchione, C.W. Garland, J.T. Mang, T.P. Rieker. *Phys. Rev. E*, **58**, 5966 (1998).
[46] P.N. Sanda, D.B. Dove, H.L. Ong, S.A. Jansen, R. Hoffmann. *Phys.Rev. A*, **39**, 2653 (1989).
[47] S. Havriliak, S. Negami. *J. polym. Sci. C*, **14**, 99 (1966).
[48] A. Kocot, R. Wrzalik, J.K. Vij, M. Brehmer, R. Zentel. *Phys. Rev. B*, **50**, 16346 (1994).
[49] S.M. Khened, S. Krishna Prasad, B. Shivkumar, B.K. Sadashiva. *J. Phys. II*, **1**, 171 (1991).